Zeitschrift: Eclogae Geologicae Helvetiae
Herausgeber: Schweizerische Geologische Gesellschaft
Band: 91 (1998)
Heft: 2

Artikel: Abrupt climatic, oceanographic and eclogic changes near the Paleocene-Eocene transition in the deep Tethys basin : the Ademilla section, southern Spain
Autor: Lu, Gangyi / Adatte, Thierry / Keller, Gerta
DOI: https://doi.org/10.5169/seals-168424

0012-9402/98/020293-14 $1.50 + 0.20/0
Birkhäuser Verlag, Basel, 1998

Eclogae geol. Helv. 91 (1998) 293–306

Abrupt climatic, oceanographic and ecologic changes near the Paleocene-Eocene transition in the deep Tethys basin: The Alademilla section, southern Spain

GANGYI LU[1], THIERRY ADATTE[2], GERTA KELLER[1] & NIEVES ORTIZ[1]

Key words: Paleocene-Eocene transition, Tethys, paleo-oceanography, paleo-climate, warming, aridity, faunal turnover, stable isotopes, clay-minerals

ABSTRACT

The Tethys is a critical region for investigating the mechanism(s) of the Paleocene-Eocene global change, because of its potential in producing warm saline water masses, a possible driving force for the deep ocean warming at this time. To examine climatic, oceanographic and ecologic changes in the deep Tethys basin, we conducted high resolution faunal, isotopic and mineralogic analyses across the P-E transition at the Alamedilla section (paleodepth between 1000 m and 2000 m) in southern Spain. At this location, foraminiferal $\delta^{18}O$ values show little temperature change in surface waters, but a 4 °C warming in bottom waters. Comparison with deep-sea sites indicates that Antarctic intermediate water was consistently colder than Tethys bottom water. During the course of the P-E global change, however, the temperature difference between these two water masses was reduced from a previous 5 °C to 3 °C. Clay mineralogic analyses at the Alamedilla section indicate increased aridity in the Tethys region that contrasts with a humid episode on Antarctica during high-latitude warming. Foraminiferal $\delta^{13}C$ values at Alamedilla show a negative excursion of 1.7‰ in both surface and bottom waters with little change in the vertical $\delta^{13}C$ gradient. Accumulation of organic and inorganic carbon in sediments decreased significantly, suggesting changes in the size and structure of the oceanic carbon reservoir. Associated with these climatic and oceanographic changes is a reorganization of the Tethys ecosystem, a benthic foraminiferal mass extinction, and planktonic foraminiferal assemblages marked by increased species turnover rates and high relative abundance of short-lived, opportunistic species that suggest increased instability.

RESUME

La Tethys est considérée comme une des régions critiques pour étudier les causes et les mécanismes du changement global ayant caractérisé la transition Paleocène-Eocène (P-E); car elle pourrait avoir constitué une source potentielle de masses d'eau profonde, chaude et saline, un des éléments moteurs du réchauffement des eaux océaniques profondes observé à cette période. Des analyses micropaléontologiques, isotopiques et minéralogiques de haute résolution, ont été menées sur la coupe d'Alamedilla (paléo-profondeur allant de 1000 à 2000 m), située dans le Sud de l'Espagne, dans le but de caractériser les changements climatiques, océanographiques et faunistiques ayant affecté la transition P-E. Dans cette section, si les valeurs de $\delta^{18}O$, mesurées sur les foraminifères, ne varient presque pas dans les eaux de surface, elles indiquent, par contre, un réchauffement de 4 °C des eaux profondes. Par comparaison avec d'autres sites océaniques, les eaux intermédiaires antarctiques étaient, par exemple, sensiblement plus froides que les eaux profondes tethysiennes. Cependant la différence de température caractérisant ces deux masses d'eaux, s'est réduite de 5 à 3 °C durant la transition P-E. Pendant ce réchauffement, la succession des minéraux argileux indique une augmentation de l'aridité dans les régions tethysiennes, alors qu'un climat humide régnait dans les hautes latitudes antarctiques. Les valeurs de $\delta^{13}C$, mesurées sur les foraminifères récoltés dans la section d'Alamedilla, montrent une excursion négative de 1.7‰, aussi bien dans les eaux de surface que dans les eaux profondes, sans changement significatif du gradient vertical. Les taux de carbone organique et inorganique diminuent drastiquement, suggérant des changements importants dans la taille et la structure du réservoir océanique. Une réorganisation de l'éco-système téthysien est associée à ces changements climatiques et océanographiques, caractérisée par une extinction massive des foraminifères benthiques, une augmentation de la diversité dans les assemblages de foraminifères planctoniques et une grande abondance d'espèces opportunistes et éphèmères, indiquant une instabilité croissante des milieux.

Introduction

A remarkable short-term global change occurred approximately 55 million years ago near the Paleocene-Eocene (P-E) transition (Cande & Kent 1992; Berggren et al. 1995). Some studies suggest that this global change took place within a few thousand years (kyr) and lasted less than 200 kyr (Kennett & Stott 1991). It is characterized by a transient climate (referred as Late Paleocene Thermal Maximum, or LPTM), drastic changes in the global carbon budget, reorganization of ecosystems, and a possible change in the thermohaline circulation in the ocean. The P-E transient climate is marked by a 6–8 °C warming in the deep ocean and high-latitude surface ocean, but little water-temperature change in the low-latitude surface

[1] Department of Geosciences, Princeton University, Princeton, NJ 08544, USA. keller@geo.Princeton.EDU
[2] Corresponding author, Institut de Géologie, 11 rue Emile Argand, CH–2007 Neuchâtel. Email: thierry.adatte@geol.unine.ch

ocean, as indicated by planktonic and benthic foraminiferal $\delta^{18}O$ values (Kennett & Stott 1991; Pak & Miller 1992; Stott 1992; Corfield & Cartlidge 1992; Lu & Keller 1993; Bralower et al. 1995; Thomas & Shackleton 1996).

Clay mineral compositions suggest a time of exceptionally high precipitation on Antarctica (Robert & Kennett 1992, 1994), but an arid climate in the Tethys region (Lu et al. 1995c; Bolle et al. 1998). Global carbon budget changes are indicated by a negative excursion of 2.5–3‰ (global average) in carbonate $\delta^{13}C$ values in the ocean (Kennett & Stott 1991; Pak & Miller 1992; Stott 1992; Lu & Keller 1993; Canudo et al. 1995; Bralower et al. 1995; Lu et al. 1995a; Thomas & Shackleton 1996) and the corresponding excursions in carbonate and organic matters on land (Koch et al. 1992, 1995; Sinha & Stott 1994; Stott et al. 1996). Coincident with the $\delta^{13}C$ excursion, carbonate sedimentation decreased drastically across all major ocean basins as well as on continental margins (O'Connell 1990; Canudo et al. 1995; Thomas & Shackleton 1996), suggesting changes in the size of the oceanic carbon reservoir, which might have affected atmospheric CO_2 concentrations. The reorganization of ecosystems associated with the P-E global change is marked by a mass extinction in benthic foraminifera (Miller et al. 1987b; Thomas 1990, 1992, in press; Katz & Miller 1991; Pak & Miller 1992; Speijer 1994a, b; Canudo et al. 1995; Kaiho et al. 1996; Thomas and Shackleton 1996), but radiation and proliferation of thermophilic species in marine plankton and terrestrial vertebrates and plants (Gingerich 1980, 1986; Wing et al. 1991; Axelrod 1992; Wing & Greenwood 1993; Lu & Keller 1993).

The LPTM represents one of the most dramatic warming events in the geological records. Surface water temperatures near Antarctica may have reached 20 °C (Kennett & Stott 1991), the highest values observed over the last 100 million years. Moreover, the rate and magnitude of the associated $\delta^{13}C$ excursion are far beyond that achieved through biotic, sedimentation, and erosion processes (Eldholm & Thomas 1993; Thomas & Shackleton 1996). Several hypotheses, ranging from enhanced hydrothermal activity on the sea floor to the sudden emission of green-house gases, have been proposed as potential causal agents of this unusual warming (Owen & Rea 1985; Rea et al. 1990; Kennett & Stott 1990, 1991; Sloan et al. 1992; Eldholm & Thomas 1993; Zachos et al. 1993; Thomas & Shackleton 1996; O'Connell et al. 1996). Among them, the warm saline deep water (WSDW) hypothesis has generated wide attention and is particularly relevant in paleoceanographic studies of the Tethys. During the P-E transition, the Tethys was a semi-restricted basin surrounded by vast areas of shallow epicontinental seas (Oberhänsli & Hsü 1986; Oberhänsli 1992; O'Connell et al. 1996). This unique geographic feature suggests that the Tethys region was potentially a major source of warm saline deep water, a possible driving force for the P-E deep ocean warming (Kennett & Stott 1990, 1991).

Recent investigations of P-E sections from continental margins of the Tethys (Spain, Tunisia, Israel and Egypt) reveal various marker events for the P-E global change, including the $\delta^{13}C$ excursion (Lu et al. 1995a; Canudo et al. 1995; Schmitz et al. 1996), benthic foraminiferal mass extinction (Speijer 1994; Ortiz 1994, 1995; Kaminski et al. 1996), and planktonic foraminiferal turnover (Canudo et al. 1995). These studies provide crucial information on the neritic to middle bathyal environment along the southern and western margins of the Tethys. However, the deep environment of the Tethys basin during the P-E interval remains largely unknown. In this study, we have sampled and analyzed the Alamedilla section from southern Spain, which formed in a lower bathyal environment. By conducting high-resolution faunal, isotopic and mineralogic analyses, we document the characteristics of the P-E events in the deep Tethys basin, correlate these events with the deep-sea records, and detail the onset of the isotopic excursion. Specifically, we intend to use clay mineralogic data to evaluate arid or humid climates, and benthic foraminiferal $\delta^{18}O$ values to evaluate deep water warming in the Tethys. We then use the carbon and oxygen isotopes to reconstruct changes in temperature and nutrient patterns between low and high latitudes intermediate water masses.

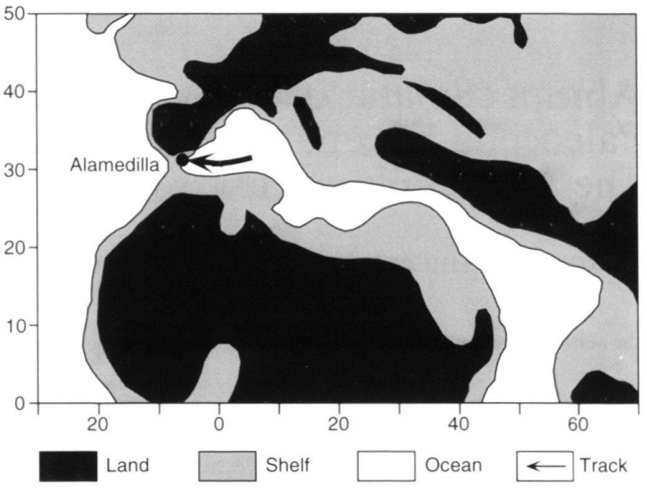

Fig. 1. A paleogeographic reconstruction at the time of the Paleocene-Eocene transition in the western Tethys region using the PGIS program. The map shows the location of the Alamedilla section and a possible path of tectonic back-tracking.

Materials and methods

Section and sampling: The Alamedilla section is located near the village of Alamedilla, in the Province of Granada, Spain, and is geologically in the Subbetic Zone (Betic Cordillera). Faunal assemblages suggest the section was within the extended tropical-subtropical zone during the P-E thermal maximum. A possible back-tracking path of the Alamedilla section is shown in Figure 1. The estimated paleodepth for the section, based on benthic foraminiferal assemblages, is between 1000 m and 2000 m (Lu et al. 1996; Ortiz unpubl. data).

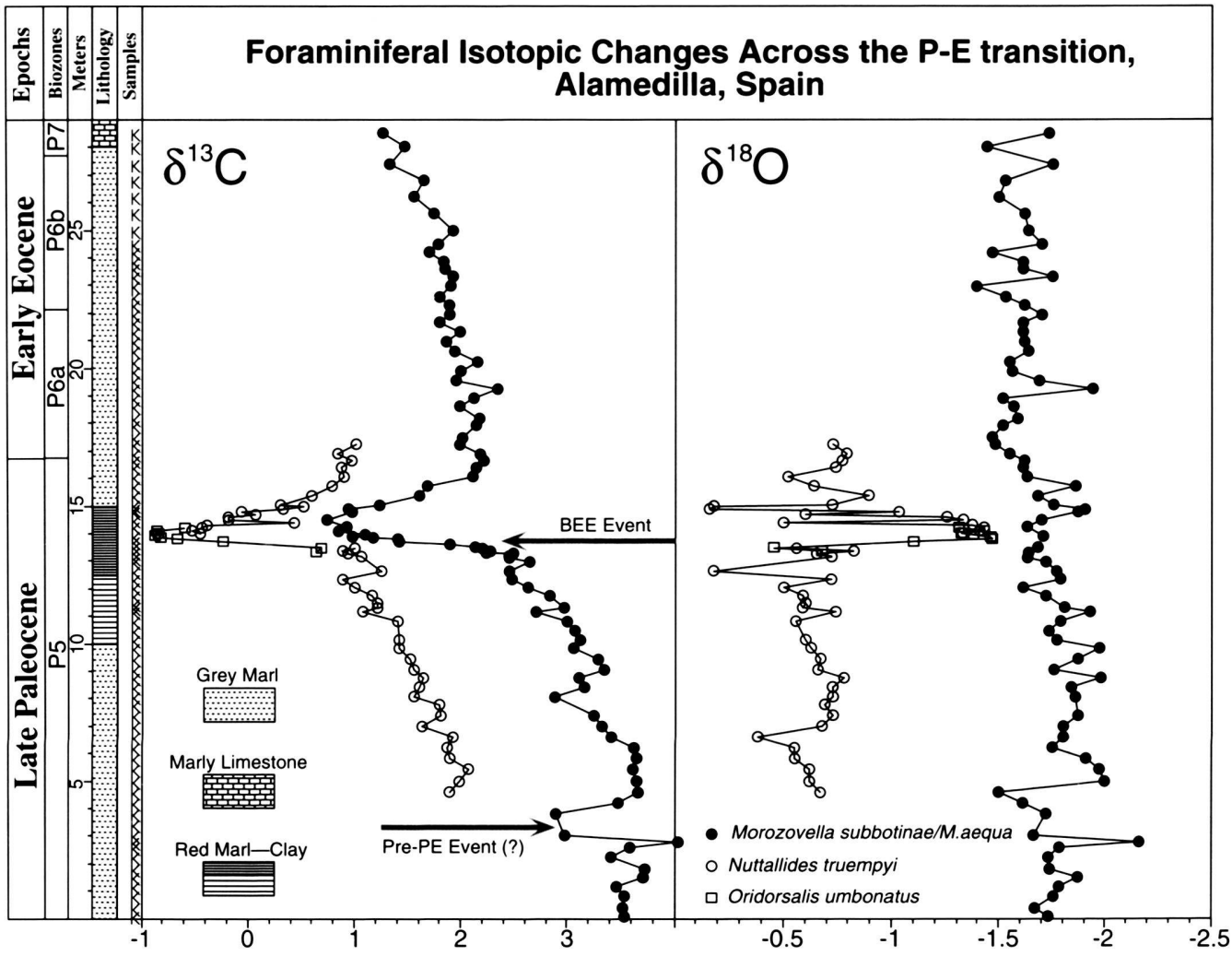

Fig. 2. Foraminiferal $\delta^{18}O$ and $\delta^{13}C$ values at the Alamedilla section. Solid dots mark planktonic values, whereas open circles and squares mark benthic values.

The base of the Alamedilla section rests on a disconformity that spans from the upper part of Zone P2 to the lower part of Zone P5 (Zonal scheme of Berggren et al. 1995). The top of the section is marked by a marly limestone layer which is stratigraphically in the lower part of Zone P7. The lower 10 m of the section consist of grey marls. Between 10 m to 15 m, grey marls grade into reddish clay. At 15 m, the red clay is replaced again by grey marls which continues through the top 13 m of the section. The section was sampled at an average of 35 cm between Zones P5 and P7 which span a total of 28 m and represent approximately 2.5 myr. In the red clay layer between 13 m and 15 m, samples were collected at 5 to 10 cm intervals.

Methods

Foraminifera: Sediments were soaked in water and washed through a 63 μm sieve. An ultrasonic bath was used to further clean the recovered foraminiferal tests. Stratigraphic ranges and relative abundance of planktonic foraminiferal species for each sample were determined from counts of a random split of about 300 foraminiferal specimens in the >106 μm size fraction. The planktonic foraminiferal zonation in this study is based on the zonation of Berggren et al. (1995). Benthic foraminifera were examined in the >63 μm size fraction to determine the position of the mass extinction.

Stable isotope: Oxygen and carbon isotope analyses were based on monospecific samples. The species *Morozovella subbotinae* was used for planktonic isotope analyses because of its surface dwelling habitat (Shackleton et al. 1985; Lu & Keller 1996), and presence in most of the studied interval. For the basal 2.5 m of sediments (7 samples) below the first stratigraphic appearance of *M. subbotinae*, the species *M. aequa*, which is similar to *M. subbotinae* in morphology and isotope signals (Lu & Keller 1996), was used for analyses. To minimize intraspecific variations, all planktonic isotope analyses used 30 specimens from the 300–355 μm size fraction.

Isotope analyses were performed on the benthic foraminifer *Nuttallides truempyi* for the interval between 4.6 m and 17.25 m. Within the interval between 13.45 m and 14.0 m, where *N. truempyi* temporarily disappears, *Oridorsalis umbonatus* was analyzed. Offsets in $\delta^{18}O$ and $\delta^{13}C$ values between the two species, based on 5 paired measurements, average 0.07‰ and 0.28‰ respectively. Each benthic isotope analysis used 40–70 specimens from the >125 μm size fraction.

Analyses were conducted at the stable isotope geochemistry laboratory at Princeton University using a VG Optima gas source mass spectrometer equipped with a common acid bath. The results were calibrated to the PDB scale with the standard errors of 0.05‰ for $\delta^{13}C$ and 0.1‰ for $\delta^{18}O$.

Mineralogical analyses: XRD analyses of whole rock and clay mineralogic analyses were conducted at the Geological Institute of the University of Neuchâtel using a SCINTAG XRD 2000 Diffractometer. Whole rock samples were prepared following the procedure of Kübler (1987). For each rock sample, approximately 20 grams were ground to obtain small rock chips (1 to 5 mm). Of these, 5 grams were dried at a temperature of 60 °C and then ground again to a homogenous powder with particle sizes <40μm. 800 mg of this powder were compressed (20 bars) in a powder holder and analyzed by XRD. Whole rock composition was determined using external standards based on the methods described by Ferrero (1965, 1966), Klug & Alexander (1974), Kübler (1983), and Moore & Reynolds (1989).

Clay mineral analyses were based on the methods by Kübler (1987). Ground chips were mixed with de-ionized water (pH 7–8) and agitated. The carbonate fraction was removed with 10% HCl (1.25 N) at room temperature for 20 minutes or more until all the carbonate was dissolved. Ultrasonic disaggregation was performed for 3 minutes. The insoluble residue was washed and centrifuged (5–6 times) until a neutral suspension was obtained (pH 7–8). Separation of different grain size fractions (<2 μm and 2–16 μm) was obtained by the timed settling method based on Stokes law. The selected fraction was then pipetted onto a glass plate and air-dried at room temperature for XRD analysis. The intensities of selected XRD peaks characterizing each clay mineral (e.g. chlorite, mica, kaolinite, palygorskite, sepiolite, smectite and illite-smectite mixed-layers) were measured for a semi-quantitative estimate of the proportion of clay minerals present in the size-fractions <2 μm and 2–16 μm. Therefore, clay minerals are given in relative percent abundance without correction factors. All data are electronically archived at NOAA.

Stratigraphy and timescale: Stratigraphic control of the Alamedilla section is based on a combination of (1) planktonic foraminiferal biostratigraphy (Berggren & Miller 1988; Lu & Keller 1995a), (2) an event horizon as defined by the benthic foraminiferal extinction and/or the onset of the $\delta^{13}C$ excursion (Kennett & Stott 1991; Thomas & Shackleton 1996), and (3) $\delta^{13}C$ stratigraphy (Kennett & Stott 1991; Stott 1992; Lu & Keller 1993; Bralower et al. 1995; Thomas & Shackleton 1996). The last appearance of *Morozovella velascoensis* is used to approximate the Paleocene/Eocene boundary which has not yet been formally designated (Berggren et al. 1985, 1995; Aubry et al. 1988, 1996). Because of the uncertainty in locating the P/E boundary in marine sediments using different stratigraphic markers, we use "P-E transition" to characterize the stratigraphic interval where the benthic foraminiferal extinction and the isotopic excursion are located. Numerical ages are based on the geomagnetic polarity time scale (GPTS) by Cande & Kent (1992), rather than the newly revised time scale by Berggren et al. (1995), in order to permit the convenience of correlating with previously published data.

Results

Isotopes

Planktonic $\delta^{13}C$ values show a long-term decrease superimposed by a short-term negative excursion (Fig. 2). This $\delta^{13}C$ trend can be divided into four major intervals which mark the progressive $\delta^{13}C$ changes across the P-E transition. Between 0 m and 6.40 m, planktonic $\delta^{13}C$ values are relatively stable at 3.6‰. However, at the 3 m level near the P5/P6a biozone boundary, $\delta^{13}C$ values decrease to 3.0‰ coincident with fluctuating planktonic $\delta^{18}O$ values (Fig. 2), a decrease in calcite content (Fig. 3), and a moderate faunal change in planktonic foraminifera (Fig. 4). The nature of this 3 m level change is not known. From 6.4 to 13.25 m, planktonic $\delta^{13}C$ values gradually decrease by 1‰. Following this gradual decrease is the interval of the P-E $\delta^{13}C$ excursion between 13.25 m and 16.05 m (Fig. 2). The onset of this excursion is recorded in a 70 cm interval between 13.25 m and 13.95 m as marked by a rapid decrease of 1.7‰. Between 13.95 m and 14.90 m, planktonic $\delta^{13}C$ values remain at the lowest level (<1‰) of the entire observed interval. A gradual recovery begins at 15.05 m and ends at 16.05 m. Above 16.05 m, planktonic $\delta^{13}C$ values decrease gradually to the top of the section.

The pattern of the benthic $\delta^{13}C$ curve is similar to the planktonic curve, including a 1.7‰ excursion between 13.45 m and 16.05 m, and a 1‰ gradual decrease prior to the excursion between 6.4 m and 13.45 m (Fig. 2). There is a 1.6‰ average gradient between planktonic and benthic $\delta^{13}C$ values, which remains nearly constant during the excursion.

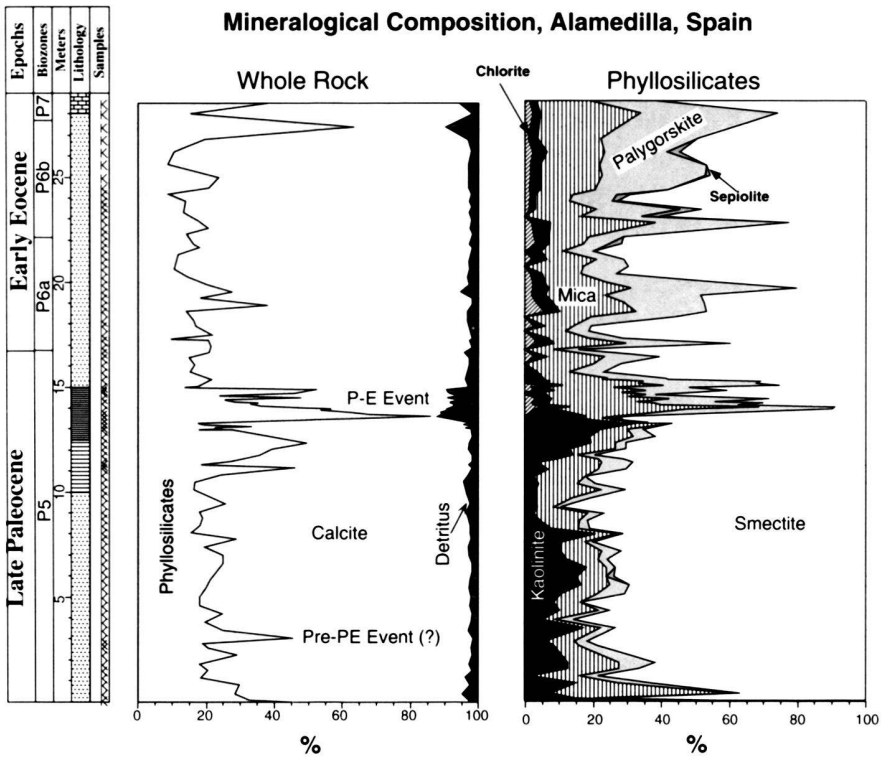

Fig. 3. Whole rock and clay mineralogic compositions at the Alamedilla section. Detritus measures the content of detrital quartz, K-feldspar and plagioclase.

Planktonic $\delta^{18}O$ values show no excursion near the P-E transition (Fig. 2). Between 0 m and 13 m, planktonic $\delta^{18}O$ values average –1.8‰. A gradual increase of 0.2‰ is observed between 13 m and 18 m, approximately over the interval of the $\delta^{13}C$ excursion. Above 18 m, planktonic $\delta^{18}O$ values average –1.6‰.

In contrast to planktonic values, benthic $\delta^{18}O$ values reveal the P-E excursion (Fig. 2). Between 4.6 m and 13.45 m, benthic $\delta^{18}O$ values average –0.63‰. An abrupt negative excursion of 0.85‰ is observed in a 35 cm interval between 13.45 m and 13.8 m. Between 13.8 m and 14.3 m, benthic $\delta^{18}O$ remain at the lowest level (<–1.3‰). These values fluctuate between 14.3 m and 15.05 m. Above 15.05 m, benthic $\delta^{18}O$ values recover to pre-excursion values with an average of –0.73‰.

Mineralogy

Whole rock analyses show that the dominant component of the sediments is calcite, which accounts for 74% in the lower part of the section (from the base to 11 m), and 78% in the upper part of the section (from 15 m to the top, Fig. 3). Between 11 m and 13.45 m, calcite fluctuates between 40% to 80%. The onset of the P-E event is marked by a dramatic decrease in calcite content to 2%. During the P-E event interval (13.45 m to 15 m), calcite content varies between 20% and 70%, and averages 44%. Changes in the percentage of calcite are primarily compensated by changes in phyllosilicates (Fig. 3). Phyllosilicates account for an average 23% in the lower part, and 19% in the upper part of the section. During the P-E event, phyllosilicate content is as high as 86%, and averages 47%. Detritus is used here to summarize three minor components, including quartz, K-feldspar and plagioclase. Detritus averages 3% from the base of the section to 13.45 m and from 15 m to the top. During the P-E event interval (13.45 m to 15 m), detritus content increases to 12% and averages 9% (Fig. 3).

Based on relative abundance changes below and above the P-E event interval, six measurable phyllosilicate species (<2 μm) can be grouped into two assemblages: 1) the pre-PE marker assemblage, which includes smectite and kaolinite, and 2) the post-PE marker assemblage, which includes mica, palygorskite, chlorite and sepiolite (Fig. 3). From the base to 13.45 m, the pre-PE marker assemblage dominates phyllosilicates (<2 μm fraction), with 70% smectite and 14% kaolinite. The post-PE marker assemblage in this interval is composed of only mica and palygorskite, and accounts for 16%. At the P-E event between 13.45 m and 15 m, the relative abundance of the pre-PE assemblage decreased to an average of 42% (37% for smectite and 5% for kaolinite) and reached a low of 15%. In contrast, the relative abundance of the post-PE marker assemblage increased to an average of 58% and reached a high of 85% (Fig. 3). Chlorite, a minor species, first appears associated with the onset of the P-E event (13.45 m). Above the P-E event (from 15 m to the top), the pre-PE assemblage

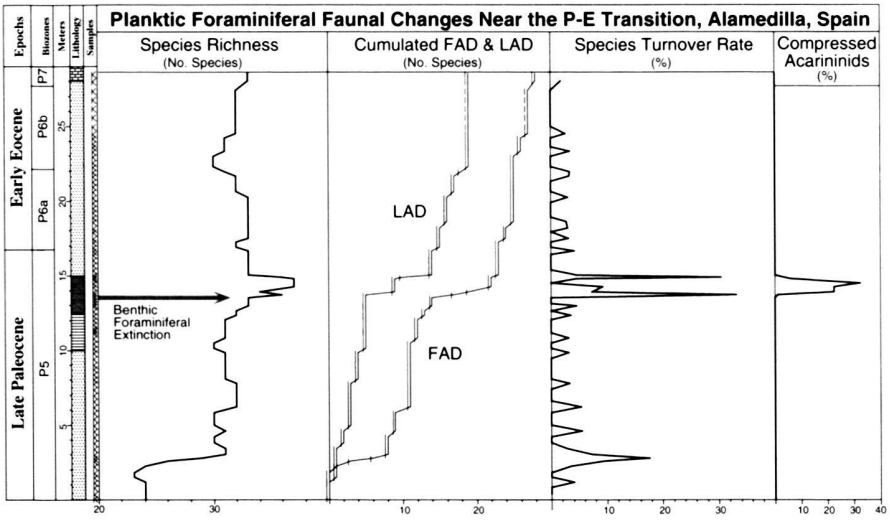

Fig. 4. Planktonic foraminiferal changes at the Alamedilla section. Species richness refers to the number of species in each sediment sample. FAD and LAD stand for first and last appearance datums, respectively. The relative species turnover rate refers to the percentage of FADs and LADs normalized to sample resolutions. Compressed acarininids include *A. africana, A. sabaiyaensis* and *A. berggreni*.

accounts for an average of 58%, with smectite, the major species, fluctuating between 20% and 80%. The post-PE assemblage accounts for 42%. Sepiolite, another minor species, also appears in this interval.

Foraminifera

Faunal changes in planktonic foraminifera can be detected at both species and population levels (Fig. 4). Species changes are demonstrated by the species richness, cumulative first appearance datums (FAD) and last appearance datums (LAD), and the relative species turnover rate. The relative species turnover rate is the percentage of the combined FADs and LADs that is normalized to the sample resolutions, and can be calculated by:

$$\frac{\text{First \& Last Appearances}}{\text{(Species Richness) * (Sample Spacing) / (Mean Sample Spacing)}} * 100$$

The P-E faunal change in planktonic foraminifera is located approximately between 13.5 m and 15 m (Fig. 4). Within this interval, species richness increased temporarily. Large numbers of first and last appearances of species (18 species) push the relative species turnover rate to its highest level (34%). The twin peaks in relative species turnover rates coincide with the onset and end of the P-E faunal change and is largely caused by the appearence and extinction of a small group of compressed acarininid species. This group of acarininid species first appears in this interval and reaches a maximum combined relative abundance of 33% (Fig. 4). The group includes three acarininid species (e.g., *A. africana, A. sabaiyaensis* and *A. berggreni*) that were first described by El-Naggar (1966) from the Esna-Idfu region of Egypt near the P-E transition. Similar species now have also been identified from ODP Site 865 in the tropical Pacific (Kelly et al. 1996). In addition, P-E faunal turnover is also marked by a major change in the composition of the population with several other species appearing and/or disappearing across the P-E transition (e.g. *Morozovella velascoensis, M. subbotinae, Igorina pusilla, I. laevigata*). But this does not appear to be related specifically to the P-E event as earlier envisaged in Arenillas & Molina (1996).

Discussion

Results of isotopic, mineralogic and faunal analyses of the Alamedilla section reveal the P-E event recorded in the deep Tethys basin (Figs. 2–4). The onset of the P-E event is synchronous for most of the indices, and is marked by an abrupt change at 13.45 m. The main phase of the event is observed in a 1.55 m interval between 13.45 m and 15 m, although the $\delta^{13}C$ excursion lasts about 2.8 m. The termination of the event is abrupt for some indices, such as benthic $\delta^{18}O$ values, relative species turnover rate, and calcite percentage, but gradual for others, such as planktonic and benthic $\delta^{13}C$ values. Some indices also show a gradual, prelude change just below the onset of the P-E event, as evident in planktonic and benthic $\delta^{13}C$, calcite, phyllosilicates, and smectite (Figs. 2 & 4). These results provide crucial information for our understanding of the climatic, oceanographic, and ecologic changes in the Tethys basin during the P-E transition. Moreover, this prelude decrease is observed in several other Spanish and Tunisian sections (Bolle et al. 1998 and submitted).

Water temperature

For an open ocean site, water temperatures can be computed using the calcite/water $\delta^{18}O$ temperature equation of Erez & Luz (1983):

$$T = 16.998 - 4.52\,(\delta^{18}O_{CC} - \delta^{18}O_{SW}) + 0.028\,(\delta^{18}OCC - \delta^{18}O_{SW})^2 \qquad (1)$$

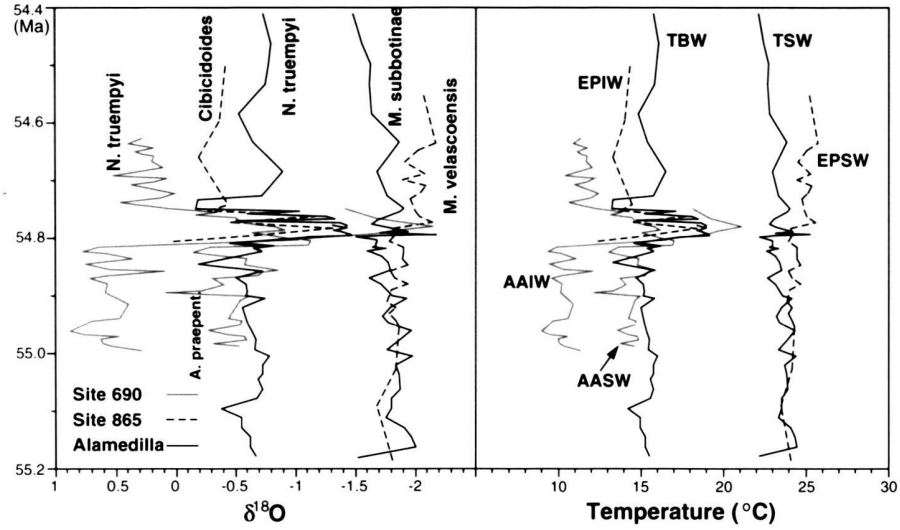

Fig. 5. Correlation of foraminiferal $\delta^{18}O$ values and estimated paleotemperatures between the Alamedilla section and deep-sea sites. Different foraminiferal species are used to measure $\delta^{18}O$ values. Possible interspecific variations in $\delta^{18}O$ values are adjusted for paleotemperature estimates. The temperature calculation is based on the equation by Erez and Luz (1983), and the systematic change in sea water $\delta^{18}O$ values across latitudes is adjusted using the equation by Zachos et al. (1994). Abbreviations: TSW – Tethys Surface Water; TBW – Tethys Bottom Water; EPSW – Equatorial Pacific Surface Water; EPIW – Equatorial Pacific Intermediate Water; AASW – Antarctic Surface Water; AAIW – Antarctic Intermediate Water.

where $\delta^{18}O_{CC}$ is the isotopic composition of foraminiferal $CaCO_3$ (PDB) and $\delta^{18}O_{SW}$ is the isotopic composition of seawater (SMOW). During P-E time, a $\delta^{18}O_{SW}$ value of –1‰ (an ice-free earth) is commonly used for computing bottom water temperatures using benthic foraminiferal $\delta^{18}O$ values (Miller et al. 1987a; Zachos et al. 1994). To compute surface water temperature using planktonic foraminiferal $\delta^{18}O$ values, systematic changes in surface ocean $\delta^{18}O_{SW}$ values as a function of latitude have to be adjusted. This can be done by using a polynomial fit to the present surface ocean $\delta^{18}O_{SW}$ profile (Zachos et al. 1994):

$$\Delta\delta^{18}O_{SW} = 0.576 + 0.041x - 0.0017\,x^2 + 1.35*10^{-5}x^3 \quad (2)$$

where $\Delta\,\delta^{18}O_{SW}$ is the deviation of $\delta^{18}O_{SW}$ values at a certain latitude from the mean $\delta^{18}O_{SW}$, and x is the latitude between 0° and 70°. However, applying this approach to semi-enclosed seas, such as the Tethys, may cause problems because their surface $\delta^{18}O_{SW}$ might deviate significantly from the global pattern (Zachos et al. 1994). It has been suggested that, during the P-E transition, enhanced evaporation might have produced a saline surface water mass, and thus higher surface $\delta^{18}O_{SW}$ values, in the Tethys (Kennett & Stott 1990, 1991; see also O'Connell et al. 1996). An oceanic general circulation model with prescribed atmospheric forcing also predict higher salinity in the Tethys basin than in open oceans for this time (Barron & Peterson 1991). Despite these considerations, we apply equations (1) and (2) to compute water temperatures in the Tethys because at present there are no other reliable ways to estimate surface $\delta^{18}O_{SW}$ values for this basin back to P-E time. We will temporarily ignore the possible anomalies in the Tethys surface $\delta^{18}O_{SW}$ values, and discuss these anomalies and their effects on water temperature estimates in the following section.

Figure 5 shows planktonic and benthic foraminiferal $\delta^{18}O$ values at the Alamedilla section for a 0.8 myr interval across the P-E isotopic excursion and calculated temperatures for surface and bottom water masses based on these $\delta^{18}O$ values using the equations (1) and (2). To compare $\delta^{18}O$ and water temperature signals between the Alamedilla section and deep-sea sites, we also plot data from the equatorial Pacific ODP Site 865 (Bralower et al. 1995) and Antarctic Site 690 (Kennett & Stott 1991) in Figure 5. Correlation between the three sections is based on $\delta^{13}C$ stratigraphy. Since the isotopic analyses of these sections used different foraminiferal species, interspecific variations in isotopic signals must be considered. Table 1 lists the related species pairs and their isotopic offsets. These data indicate that $\delta^{18}O$ differences for the species pairs used in these studies are close to the measurement errors and have little effect on water temperatures.

Comparison of raw $\delta^{18}O$ values between the Alamedilla section and Site 865 shows a similar pattern in that there is only a minor (~0.5 permil) excursion in planktonic $\delta^{18}O$ values, but a major negative excursion in benthic $\delta^{18}O$ values (Fig. 5). During the P-E transition, Site 865 was located near the equator, whereas the Alamedilla section was at approximately 30°N (Fig. 1). The similarity in planktonic $\delta^{18}O$ values between these two sections indicates an expanded tropical zone relative to the Recent. Between 55.2 Ma and 55 Ma, apparent water temperatures are similar (24 °C) for the Tethys Surface Water (TSW) and the Equatorial Pacific Surface Water (EPSW). After 55 Ma, the two temperature curves depart from each other as the results of gradual cooling in the TSW and a gradual warming in the EPSW (Fig. 5). After the LPTM, temperatures of these two water masses differ by 3 °C. An alternative explanation for the departure between the two curves is a change in salinity/$\delta^{18}O_{SW}$. For instance, an increase in salinity/$\delta^{18}O_{SW}$ in the Tethys can produce the appearance of a cooling. On a broader scale, a salinity increase in low latitude surface waters might have dampened any warming signals recorded in $\delta^{18}O_{SW}$ during LPTM (Zachos et al. 1994).

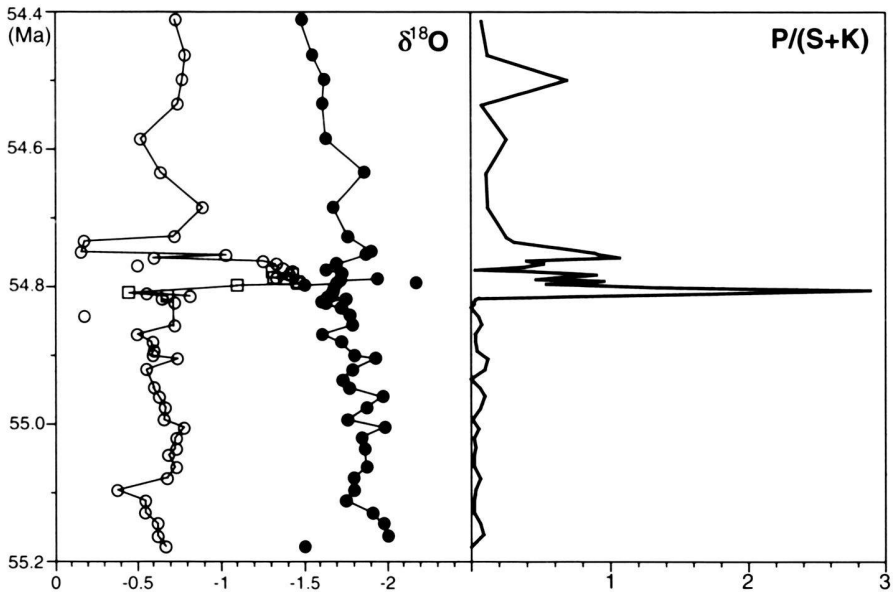

Fig. 6. Association between the benthic $\delta^{18}O$ excursion and the increase in the ratio of palygorskite and smectite-kaolinite at the Alamedilla section. This P/(S+K) ratio increase suggests increased aridity in the Tethys region.

For the intervals before and after LPTM, the temperature of the Tethys Bottom Water (TBW) is 15 °C. During LPTM, the temperature of this water mass increases to 19 °C, and thus reduces the temperature difference between the TSW and the TBW to 5 °C (Fig. 5). The onset and termination of the P-E warm event appears to be abrupt relative to the sample resolution (~5 kyr). Limited data from Site 865 indicate that the Equatorial Pacific Intermediate Water (EPIW) is 2–3 °C colder than the TBW at the beginning and after the LPTM. During the LPTM, however, the thermal characteristics of these two water masses are similar, suggesting a similar source.

Comparison of raw $\delta^{18}O$ values between the Alamedilla section and the high-latitude Site 690 shows different patterns in that 1) the negative excursion in planktonic $\delta^{18}O$ values at Site 690 is much larger than observed at the Alamedilla section, 2) both planktonic and benthic $\delta^{18}O$ values between the two sections differ by >1‰ before and after the LPTM (Fig. 5), 3) the $\delta^{18}O$ differences between the two sections is reduced significantly during the LPTM, and 4) vertical thermal gradients were reduced at both sections as the result of deep water warming. For the intervals before, during, and after the LPTM, the Antarctic Intermediate Water (AAIW) remains the coldest water mass (Fig. 5). The temperature difference between the AAIW and TBW is about 5 °C prior to the warm event and reduces to about 3 °C during the warm event. This reduction might have favored TBW over AAIW as a temporary deep water source during the LPTM.

Aridity changes

The Tethys and adjacent peri-continental basins have been regarded as a region where evaporation exceeded precipitation during the Paleogene (Brass et al. 1982; Oberhänsli & Hsü 1986; Kennett & Stott 1990; Oberhänsli 1992). Evidence for intense evaporation include evaporite deposits in northern Africa and western Europe (Millot 1970; Chamley 1989; Oberhänsli 1992) and simulation results of the atmospheric general circulation models (Barron 1985). Such climatic features might also be significant in searching for the cause(s) and mechanism(s) for the P-E short-term oceanographic changes. It has been suggested that the production of a warm saline deep water, possibly from the Tethys basin, might have increased temporarily during the P-E warming event, and thereby led to a fundamental change in thermohaline circulation (Kennett & Stott 1991; Pak & Miller 1992; Bralower et al. 1995). Signals of regional aridity changes may, therefore, help in evaluating the warm saline deep water hypothesis.

Detrital clay mineral compositions in marine sediments reflect changes in sediment source and environment of sedimenation and provide qualitative signals of regional climatic changes (Millot 1970; Windom 1976; Chamley 1989). Clay distribution patterns have been used to infer regional precipitation-evaporation changes during the Paleogene warm climate (Robert & Chamley 1991; Robert & Kennett 1992). For example, at Antarctic Site 690, the LPTM is composed essentially of smectite (90–95%) and kaolinite (5–10%) (Robert & Kennett 1994). Illite and other species occur in trace amounts. Such a clay assemblage records a subtropical humid episode on Antarctica during the LPTM (Robert & Kennett 1994). In contrast, at the subtropical Alamedilla section, the clay composition of the LPTM interval is marked by decreased relative abundance of smectite and kaolinite (Fig. 3). The percentage of palygorskite, a marker species for the subtropical arid climate, increased from 5% to 26%.

The nature of this clay composition change at Alamedilla can be illustrated by the ratio between arid clay species (paly-

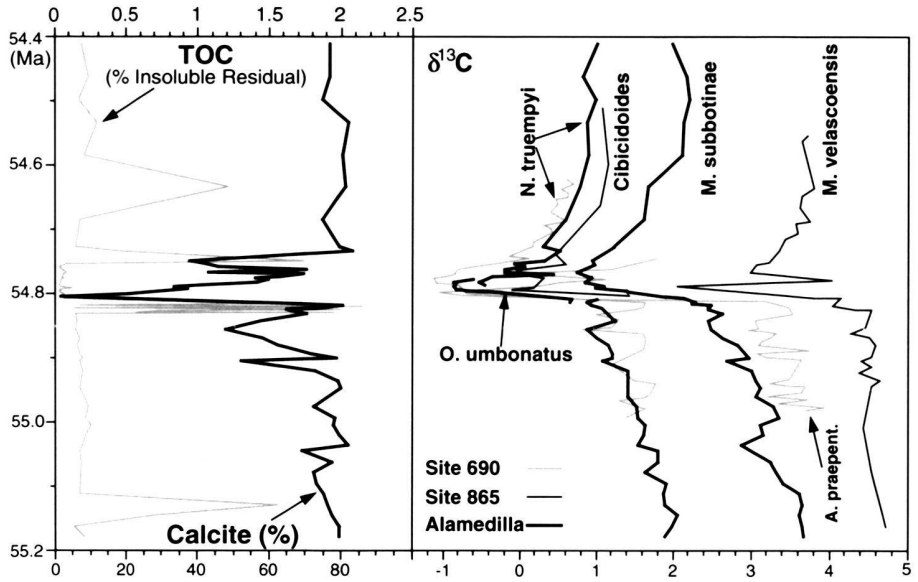

Fig. 7. Association between $\delta^{13}C$ excursion and changes in organic and inorganic carbon accumulation at the Alamedilla section. Calcite accumulation is shown as percentage of bulk sediments. TOC accumulation is shown as percentage of insoluble residuals. Also shown in the figure is a correlation of the $\delta^{13}C$ excursion with deep-sea sites. Note that different foraminiferal species are used to measure $\delta^{13}C$ values at the various deep-sea sites.

gorskite) and humid clay species (smectite and kaolinite, Fig. 6). Prior to the $\delta^{18}O$ excursion in benthic foraminifera, the P/(S+K) ratio averages less than 0.1, but during the $\delta^{18}O$ excursion, this ratio increases to an average of 0.8 and reaches a maximum of 2.9. This dramatic change in the P/(S+K) ratio suggests a marked increase in aridity on the adjacent continents of the Tethys during LPTM. After the excursion, the P/(S+K) ratio fluctuates with episodic high values, suggesting increased instability in the precipitation-evaporation balance in the Tethys region (Figs. 3 and 6).

Most of the modeling investigations for the so-called "equable climate" during the P-E transition have focused on temperature changes and heat transport (Barron 1987; Sloan & Barron 1990, 1992; O'Connell et al. 1996; Sloan & Thomas in press). Investigation of hydrologic activities during warming episodes is hampered by the lack of geological proxy, despite the central role of water in climate changes (Barron et al. 1989). Comparison of the clay composition between the Alamedilla section and Site 690 provides information on precipitation-evaporation changes during LPTM. This interval is characterized by increased aridity on the subtropical continents adjacent to the Tethys (Fig. 6), but increased humidity on Antarctica (Robert & Kennett 1994). Such a pattern suggests an increase in the pole-ward moisture transport by the atmosphere. This is interesting because climatic models have predicted a weak atmospheric circulation and reduced heat transport through the atmosphere during a time of reduced equator-to-pole temperature gradients (Barron 1987; Barron et al. 1989; Sloan & Barron 1990, 1992). How the additional moisture has been transported remains a mystery.

Moreover, the evidence of increased aridity in the Tethys region during LPTM also raises concerns about our paleotemperature estimates using foraminiferal $\delta^{18}O$ values. Paleotemperature estimates for the Tethys are limited by the uncertainty in $\delta^{18}O_{SW}$ values which might have departed significantly from the global "steady state" pattern. Since the absolute values of $\delta^{18}O_{SW}$ and its quantitative relationship with salinity can not be determined precisely, the absolute values of the paleotemperature for the Alamedilla section shown in Figure 5 should be treated with caution; they may underestimate true temperatures. Moreover, climatic interpretations of clay data may not be conclusive because of diverse authigenic conditions and transport. Other indices should therefore be examined to verify these interpretations.

Oceanic carbon reservoir

During the LPTM, the oceanic carbon reservoir changed dramatically as indicated by the $\delta^{13}C$ excursion and decreased carbonate preservation in various ocean basins (Kennett & Stott 1991; Pak & Miller 1992; Stott 1992; Lu & Keller 1993; Lu et al. 1995a; Canudo et al. 1995; Bralower et al. 1995; Stott et al. 1996; Thomas & Shackleton 1996). Associated with this oceanic change was a change in terrestrial carbon reservoir and, possibly, a change in the atmospheric CO_2 concentration (Koch et al. 1995, 1995; Stott 1992; Sinha & Stott 1994). The nature and tempo of these reservoir changes has been discussed extensively (Kennett & Stott 1991; Sloan et al. 1992; Eldholm & Thomas 1993; Zachos et al. 1993; Thomas & Shackleton 1996). Foraminiferal $\delta^{13}C$ values and bulk sediment TOC and calcite contents from the Alamedilla section provide additional evidence for further discussion (Fig. 7).

The $\delta^{13}C$ excursion includes a rapid onset, an interval of minimum $\delta^{13}C$ values, and a gradual recovery in various ocean basins (Fig. 7). The onset of the $\delta^{13}C$ excursion can be examined in detail at Alamedilla. Figure 8 shows that the $\delta^{13}C$ ex-

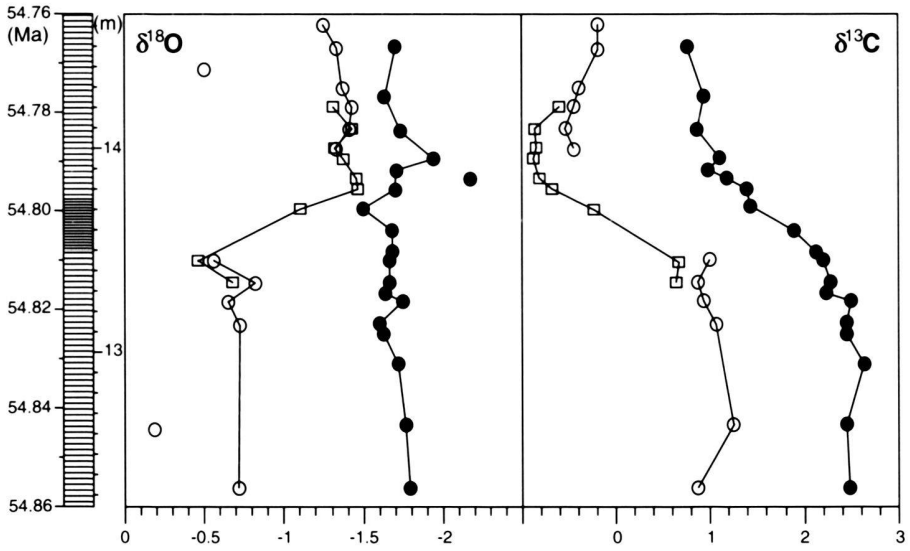

Fig. 8. Expanded interval detailing the onset of the $\delta^{18}O$ and $\delta^{13}C$ excursions at the Alamedilla section. Solid dots mark planktic forminiferal values, open circles and squares mark benthic foraminiferal values.

cursion in planktonic foraminifera occurs gradually within 70 cm of sediments and slightly leads the decrease in oxygen isotope values in benthic foraminifera. This may suggest that changes in the carbon cycle may have preceded large-scale deep water warming.

There are fewer benthic $\delta^{13}C$ data points because insufficient benthic foraminiferal specimens are available for isotopic analyses between 13.45 m to 13.7 m. Nevertheless, available data show no apparent change in the planktonic-to-benthic $\delta^{13}C$ difference during the course of the excursion at Alamedilla (Fig. 7 and 8). Such a pattern indicates: 1) well-stratified surface bottom water masses in the Tethys despite the reduction in the vertical thermal gradient as shown by $\delta^{18}O$ values (Fig. 8), 2) a parallel change between the surface and deep ocean carbon reservoirs, and 3) little change in the biological pump in the Tethys. This pattern is similar to the pattern revealed at the equatorial Pacific Site 865, but differs from the pattern at Antarctic Site 690 where a major reduction in the vertical $\delta^{13}C$ gradient has been recorded (Fig. 7).

Comparison of $\delta^{13}C$ values between different sites must consider interspecific variations in foraminiferal $\delta^{13}C$ signals. Figure 9 shows a correlation of foraminiferal $\delta^{13}C$ values between the Alamedilla section and deep-sea Sites 690 and 865 where values have been adjusted for the interspecific differences based on data in Table 1. The $\delta^{13}C$ differences of most species pairs in Table 1 are relatively small except for the *Morozovella subbotinae* and *Acarinina praepentacamerata* pair. At low latitudes, the large $\delta^{13}C$ offset in this species pair has been well documented. Another reference value for this offset is an average 0.5‰ difference in $\delta^{13}C$ values between discoidal morozovellids and rounded acarininids (Lu & Keller 1996). (Data are not available to test the $\delta^{13}C$ difference between low-latitude and high-latitude *A. praepentacamerata* in paired samples.) However, such an offset value (0.63‰, Tab. 1) should be qualitatively correct because morozovellid species consistently record heavier $\delta^{13}C$ values than acarininid species at all latitudes (Shackleton et al. 1985; Pearson et al. 1993; D'Hondt et al. 1994; Lu & Keller 1996). The $\delta^{13}C$ offset at Alamedilla between *Nuttallides truempyi* and *Oridorsalis umbonatus* is 0.28‰ based on five paired measurements. In Figure 9, all benthic $\delta^{13}C$ values are adjusted to values of *Nuttallides truempyi,* and all planktonic $\delta^{13}C$ values are adjusted to values of *Morozovella velascoensis.*

Benthic $\delta^{13}C$ values have been used to trace the source of deep water and the distance from the source (Kroopnick 1985). Similar benthic $\delta^{13}C$ values between the Alamedilla section and Site 865 during the isotopic excursion suggest uniform deep water between the Tethys and the tropical Pacific (Fig. 9), an observation also supported by the similar benthic $\delta^{18}O$ values (Fig. 5). Small $\delta^{13}C$ differences exist between Site 690 and the two low-latitude sites as shown by the heavier (< 0.3‰) values at Site 690 prior the excursion and the lighter (< 0.3‰) values at Site 690 during the excursion. This reversal in the benthic $\delta^{13}C$ gradient between high and low latitudes has been viewed as evidence of a possible change in the main deep water source(s) to low latitudes during LPTM (Katz & Miller 1991; Pak & Miller 1992; Bralower et al. 1995). Alternatively, the light benthic $\delta^{13}C$ values at Site 690 could be a result of changing local upwelling and/or productivity (Thomas & Shackleton 1996).

Comparison of planktonic $\delta^{13}C$ values reveals significant differences between the Alamedilla section and deep-sea sites (Fig. 9). Before and after the $\delta^{13}C$ excursion, planktonic $\delta^{13}C$ values at Alamedilla are 1–2‰ lighter than in the deep-sea, suggesting a nutrient-rich surface water-mass in the Tethys. Possible causes for the light $\delta^{13}C$ values include: 1) upwelling along the southern margin of the Tethys driven by the northern hemisphere tradewinds, 2) input of organic carbon from

Table 1. Offsets in isotopic signals between species pairs (*Morozovella subbotinae – Morozovella velascoensis, Morozovella subbotinae – Acarinina praepentacemerata,* and *Nuttallides truempyi – Cibicidoides* spp.).

Environ.	Species		Size (μm)	Offset*		Reference
	Alamedilla	Site 865		$\delta^{18}O$	$\delta^{13}C$	
Planktic	*M. subb.*	*M. velas.*	300–355	0.03	–0.04	Shackleton et al., 1985
	M. subb.	*A. praep.*	>300	–0.02	0.63	Lu & Keller, 1996
Benthic	*N. truem.*	*Cibicid.*	unknown	–0.12	–0.23	Pak & Miller, 1992

* Offsets are expressed as ($\delta_{M.sub} - \delta_{M.vel}$), ($\delta M.sub - \delta_{A.praep}$), and ($d_{N.t} - d_{Cib}$) for both $\delta^{18}O$ and $\delta^{13}C$ values.

the adjacent continents and epicontinental seas, and 3) a less effective biological pump in transporting light carbon to the deep water. During the $\delta^{13}C$ excursion, the planktonic $\delta^{13}C$ difference remains between the Tethys and equatorial Pacific. In contrast, planktonic $\delta^{13}C$ values at Site 690 show a much greater excursion and record the lightest planktonic $\delta^{13}C$ values during the excursion interval. Thomas & Shackleton (1996) attributed this large excursion in planktonic $\delta^{13}C$ values and the reduction in the planktonic-to-benthic $\delta^{13}C$ gradient at Site 690 partly to intense upwelling and changes in local productivity.

The P-E $\delta^{13}C$ excursion coincides with an apparent global reduction in carbonate accumulation as evidenced by: 1) decreased calcite content from an average 80% to as low as 2% at the Alamedilla section (Fig. 7), 2), decreased calcite content from an average 90% to less than 70% at Site 690 (O'Connell 1990), 3) carbonate dissolution at Site 738 (Lu & Keller 1993), 4) a condensed $\delta^{13}C$ excursion interval or a hiatus at many other deep-sea sites (Pak & Miller 1992; Bralower et al. 1995; Stott et al. 1996; Aubry et al. 1996; Thomas & Shackleton 1996), and 5) carbonate dissolution or hiatuses at many continental margin sections (Gibson et al. 1993; Canudo et al. 1995). This reduction in carbonate accumulation is abrupt and severe at the horizon of the benthic foraminiferal extinction and the onset of the $\delta^{13}C$ excursion that is usually marked by nearly complete dissolution of carbonate or a short hiatus, and followed by a gradual recovery (Fig. 7). The reduction occurs over a wide depth range from continental margins to abyssal basins. The cause(s) and mechanism(s) of this reduction are not well understood.

Ecologic changes

The P-E global change is associated with a major ecological reorganization that is highlighted by the mass extinction in benthic foraminifera (Miller et al. 1987b; Thomas 1990, 1992 in press; Katz & Miller 1991; Pak & Miller 1992; Speijer 1994a, b; Canudo et al. 1995; Ortiz 1995; Thomas & Shackleton 1996). Surface organisms react differently from benthos. Marine plankton, land mammals and plants are characterized by radiation and proliferation of thermophilic species (Gingerich, 1980, 1986; Wing et al. 1991; Axelrod 1992; Wing & Greenwood 1993; Lu & Keller 1993). In planktonic foraminifera, species richness in the tropical-subtropical Pacific increased by nearly 50% during the Paleocene-Eocene transition (Lu & Keller 1995a, b; Arenillas & Molina 1996). Evidence also suggests regional productivity changes associated with the P-E climatic and oceanographic events (Kennett & Stott 1991; Thomas & Shackleton 1996). At the Alamedilla section, foraminiferal $\delta^{13}C$ values, TOC contents in bulk sediments, and faunal analyses of planktonic foraminifera provide new constraints on the ecological changes in the Tethys basin during the P-E global change.

The mass extinction in benthic foraminifera has been a marker event for the P-E global change (Kennett & Stott 1991; Thomas 1992; Pak & Miller 1992; Zachos et al. 1993; Thomas & Shackleton 1996). However, the cause of this mass extinction is less certain. Kennett & Stott (1991) summarized three hypotheses, including: 1) the warming hypothesis – a rapid warming of the deep ocean; 2) the anoxia hypothesis – an oxygen deficiency in the deep water due to the sudden warming and a possible change in thermohaline circulation; and 3) the productivity hypothesis – a sharp drop in surface ocean productivity that reduced trophic resources available for deep-sea benthic organisms. The warming hypothesis is supported by the close association between the mass extinction and the onset of deep water warming (Kennett & Stott 1991; Pak & Miller 1992; Thomas 1992; Lu & Keller 1993; Lu et al. 1995a; Canudo et al. 1995; Bralower et al. 1995; Thomas & Shackleton 1996). The anoxia hypothesis is supported by the observation that the mass extinction is characterized by the preferential removal of epifaunal species at many sections (Thomas 1990, 1992; Kaiho 1991). One support for the productivity hypothesis is a major reduction in the planktonic-to-benthic $\delta^{13}C$ gradient at Site 690 (Kennett & Stott 1991; Thomas & Shackleton 1996). Thomas & Shackleton (1996) noticed the wide differences in composition of post-extinction faunas and suggested that regional factors might have been important in shaping the extinction patterns.

At the Alamedilla section, the mass extinction coincides with a 4 °C increase in bottom water temperatures as indicated by the excursion in benthic $\delta^{18}O$ values (Fig. 5). Such a warming would almost certainly have reduced the oxygen level. Delivery of organic particles to the bottom might have decreased significantly at this site as suggested by a reduction of TOC content in bulk sediments (Fig. 7). Prior to the mass

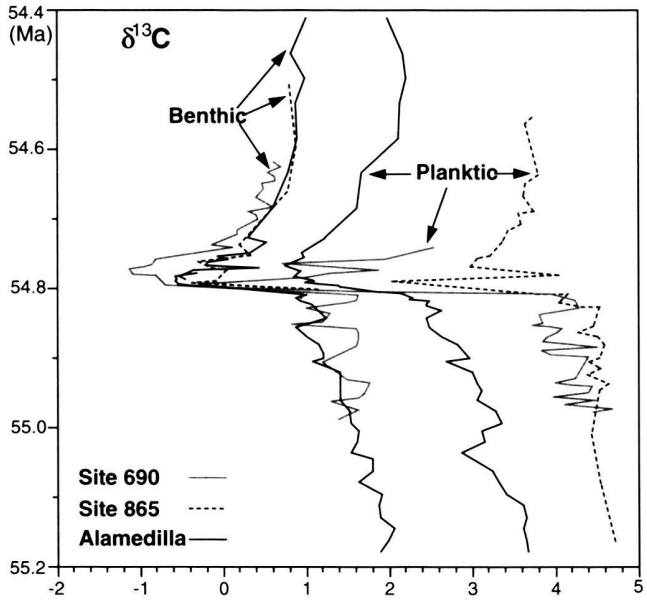

Fig. 9. Correlation of the $\delta^{13}C$ excursion between the Alamedilla section and deep-sea Sites 690 and 865 with adjusted $\delta^{13}C$ values for interspecific variations. Planktic $\delta^{13}C$ values are adjusted to the values of *Morozovella velascoensis*, whereas benthic $\delta^{13}C$ values are adjusted to the values of *Nuttallides truempyi*.

extinction and the isotopic excursion, the TOC content in insoluble residues averages nearly 0.2%. This value drops to 0.05% during the isotopic excursion and is associated with a major reduction in calcite content. Reduction in organic particle delivery to the bottom may be the result of decreased surface productivity or reduced downward particle transport. In any case, a stable planktonic-to-benthic $\delta^{13}C$ gradient during the entire course of the isotopic excursion precludes major accumulation of nutrients in the surface water mass (Fig. 8).

The plankton community in the Tethys might have undergone a significant restructuring as indicated by the faunal change in planktonic foraminifera (Fig. 4; see also Arenillas & Molina 1996). Relative species turnover rates increased dramatically, suggesting increased instability of the community. During the interval of this faunal change, short-lived opportunistic species (e.g., compressed acarininids) increased in their relative abundance (Fig. 4). Similar opportunistic species have also been observed at the equatorial Pacific Site 865 within the isotopic excursion interval (Kelly et al., 1996). These opportunistic species are marked by their dwarfed size and unique morphology. More than 50% of the low-latitude species are replaced after the P-E faunal change (Fig. 4; Lu & Keller 1995b).

Since there is little evidence of changing surface water temperatures at low latitudes, other factors, such as nutrient level, salinity, and/or water stratification, might have played important roles in the ecological changes in the Tethys plankton community. These changes might have affected the bottom water environment, as suggested by the reduction in TOC and calcite contents in sediments. It is not clear, however, whether changes in the plankton community directly affected the mass extinction in benthic foraminifera.

Conclusions

Faunal, isotopic and mineralogic analyses from the Alamedilla section reveal the following climatic, oceanographic and ecologic changes in the deep Tethys basin during the P-E global change.

1) Foraminiferal $\delta^{18}O$ values indicate that Tethys surface water temperatures ranged between 22–24 °C, and changed little during the LPTM. Tethys bottom water temperatures were close to 15 °C before and after the LPTM, but increased by 4 °C during this event. This bottom water warming resulted in a significant reduction in the vertical thermal gradient in the Tethys basin.
2) Clay mineralogic analysis at the Alamedilla section indicates a major increase in the ratio of palygorskite to smectite and kaolinite during the LPTM. This suggests increased aridity on the continents adjacent to the Tethys during the P-E transition warming event.
3) Foraminiferal $\delta^{13}C$ analysis at the Alamedilla section indicates an excursion of 1.7‰ in both planktonic and benthic values with little change in the vertical $\delta^{13}C$ gradient. The onset of this excursion is gradual and recorded in a 70 cm thick sediment layer.
4) Associated with the $\delta^{13}C$ excursion, carbonate accumulation at Alamedilla was reduced from an average of 80% to as low as 2%.
5) During the LPTM, planktonic foraminifera indicate a rapid turnover whereas benthic foraminifera suffered a mass extinction.

Acknowledgments

We thank D. Schrag and P. Koch for many discussions and conducting stable isotope measurements in the stable isotope geochemistry laboratory of Princeton University, and J. Richard from the University of Neuchâtel for the preparation of XRD samples. We thank J. Zachos, L. Derry and E. Thomas, for many suggestions in the revision of an earlier version of that manuscript. We thank also the reviewers, R. Corfield and R. Pearson for helpfull suggestions. We thank E. Molina, Zaragoza University, for providing the Alademilla section samples. This study was supported by NSF grant OCE-9021338 and Swiss National Fund No. 8220-028367.

REFERENCES

Arenillas, I. & Molina, E. 1996: Bioestratigrafía y evolucíon de las asociaciones de foraminíferos planctónicos del tránsito Paleocene-Eocene en Alamedilla (cordilleras Béticas). Rev. Esp. Micropal. 18, 85–98.

Aubry, M. P., Berggren, W. A., Kent, D. V., Flynn, J. J., Klitgord, K. D., Obradovich, J. D. & Prothero, D. R. 1988: Paleogene geochronology: An integrated approach. Paleoceanography 3, 707–742.

AUBRY, M. P., BERGGREN, W. A., STOTT, L. D. & SINHA, A. 1996: The upper Paleocene–lower Eocene stratigraphic record and the Paleocene/Eocene boundary carbon isotope excursion. J. Geol. Soc. London, Spec. Publ. 101, 353–380.

AXELROD, D. I. 1992: What is an equable climate? Palaeogeogr. Palaeoclimatol. Palaeoecol. 91, 1–12.

BARRON, E. J. 1985: Explanations of the Tertiary global cooling trend. Palaeogeogr. Palaeclimatol. Palaeoecol. 50, 45–62.

– 1987: Eocene equator-to-pole surface ocean temperatures: A significant climate problem? Paleoceanography 2, 729-739.

BARRON, E. J., HAY, W. W. & THOMPSON, S. 1989: The hydrologic cycle: a major variable during earth history. Palaeogeogr. Palaeoclimatol. Palaeoecol. 75, 157–174.

BARRON, E. J. & PETERSON, W. H. 1991: The Cenozoic ocean circulation based on General Circulation Model results. Palaeogeogr. Palaeoclimatol. Palaeoecol. 83, 1–18.

BERGGREN, W. A., KENT, D. V. & FLYNN, J. J. 1985: Paleogene geochronology and chronostratigraphy, in Geochronology and the Geological Record (ed. by N. J. SNELLING), Geol. Soc. Mem. 10, 211–260

BERGGREN, W. A., KENT, D. V., SWISHER III, C. C. & AUBRY, M. P. 1995: A revised Ceonozoic geochronology and chronostratigraphy. In Geochronology, Time Scales and Global Stratigraphic Correlation, edited by, W. A. BERGGREN, D. V. KENT, M. P. AUBRY & J. HARDENBOL, Soc. Econ. Paleont. Mineral., Spec. Publ. 54; 129–212.

BERGGREN, W. A. & MILLER, K. G. 1988: Paleogene planktonic foraminiferal biostratigraphy and magnetobiostratigraphy. Micropaleontology 34, 362–380.

BOLLE, M-P., ADATTE, T., KELLER, G. & VON SALIS, K. 1998: Stratigraphy, mineralogy and geochemistry of the Trabukua Pass and Ermua sections in Spain: Paleocene-Eocene Transition. Eclogae geol. Helv. 91, 1–25.

BOLLE, M-P., ADATTE, T., KELLER, G., VON SALIS, K. & BURNS, S. Submitted: Climatic and sea level fluctuations in the Southern Tethys (Tunisia) during the Paleocene-Eocenetransition. Bull. Soc. Géol. France.

BRALOWER, T. J., ZACHOS, J. C., THOMAS, E., PARROW, M., PAUL, C. K., KELLY, D. C., PREMOLI SILVA, I., SLITER, W. V. & LOHMANN, K. C. 1995: Late Paleocene to Eocene paleoceanography of the equatorial Pacific Ocean: Stable isotopes recorded at Ocean Drilling Program Site 865, Allison Guyot. Paleoceanography 10, 841–865.

BRASS, G. W., SOUTHAM, J. R. & PETERSON, W. H. 1982: Warm saline bottom water in the ancient ocean. Nature 296, 620–623.

CANDE, S. C. & KENT, D. V. 1992: A new geomagnetic polarity time scale for the Late Cretaceous and Cenozoic. J. Geophys. Res. 97, 13917–13951.

CANUDO, J. I., KELLER G., MOLINA, E. & ORTIZ, N. 1995: Planktic foraminiferal turnover and $\delta^{13}C$ isotopes across the Paleocene-Eocene transition at Caravaca and Zumaya, Spain. Palaeogeogr. Palaeoclimatol. Palaeoecol. 114, 75–100.

CHAMLEY, H. 1989: Clay sedimentology. Springer-Verlag, Berlin, 623 p.

CORFIELD, R. M. & CARTLIDGE, J. E. 1992: Oceanographic and climatic implications of the Palaeocene carbon isotope maximum. Terra Nova 4, 443–455.

D'HONDT, S., ZACHOS, J. C. & SCHULTZ, G. S. 1994: Stable isotopic signals and photosymbiosis in Late Paleocene planktic foraminifera. Paleobiology 20, 391–406.

EL-NAGGAR, Z. R. 1966: Stratigraphy and planktonic foraminifera of the Upper Cretaceous–Lower Tertiary succession in the Esna-Idfu region, Nile Valley, Egypt. U. A. R. British Mus. (Nat. Hist.), Bull., London, Geol. Suppl., No. 2.

ELDHOLM, O. & THOMAS, E. 1993: Environmental impact of volcanic margin formation. Earth Planet. Sci. Lett. 117, 319–329.

EREZ, J. & LUZ, B. 1983: Experimental paleotemperature equation for planktonic foraminifera. Geochim. cosmochim. Acta 47, 1025–1031.

FERRERO, J. 1965: Dosage des principaux minéraux des roches par diffraction de Rayon X. Rapport C.F.P. (Bordeaux), inédit.

– 1966: Nouvelle méthode empirique pour le dosage des minéraux par diffraction R.X. Rapport C.F.P. (Bordeaux), inédit.

GIBSON, T. G., BYBELL, L. M. & OWENS, J. P. 1993: Latest Paleocene lithologic and biotic events in neritic deposits of southwestern New Jersey. Paleoceanography 8, 495–514.

GINGERICH, P. D. 1980: Evolutionary patterns in early Cenozoic mammals. Ann. Rev. Earth Planet. Sci. 8, 407–424.

– 1986: Evolution and the fossil record: patterns, rates and processes. Canad. J. Zoology 65, 1053–1060.

KAIHO, K. 1991: Global changes of Paleogene aerobic/anaerobic benthic foraminiferal and deep-sea circulation. Palaeogeogr. Palaeclimatol. Palaeoecol. 83, 65–86.

KAIHO, K., ARINOBU, T., ISHIWATARI, R., MORGANS, H. E., OKADA, H., TAKEDA, N., TAZAKI, K., ZHOU, G., KAJIWARA, Y., MATSUMOTO, R., HIRAI, A., NIITSUMA, N. & WADA, H. 1996: Latest Paleocene benthic foraminiferal extinction and environmental changes at Tawanui, New Zealand. Paleoceanography 11, 447–465.

KAMINSKI, M. A., KUHNT, W. & RADLEY, J. 1996: Paleocene-Eocene deep-water agglutinated foraminifera from the Numidian Flysch (Rif, Northern Morocco): their significance for the palaeoceanography of the Gibraltar gateway. J. Micropaleontology 15, 1–19.

KATZ, M. E. & MILLER, K. G. 1991: Early Paleogene benthic foraminiferal assemblages and stable isotopes in the Southern Ocean. Proc. ODP, Sci. Results 114, 481–512.

KELLY, D. C., BRALOWER T. J., ZACHOS J. C., THOMAS E. & PREMOLI I. SILVA, 1996: Rapid diversification of planktonic foraminifera in the tropical Pacific (ODP Site 865) during the late Paleocene thermal maximum. Geology 24, 423–426.

KENNETT, J. P. & STOTT, L. D. 1990: Proteus and Proto-Oceanus: Paleogene oceans as revealed from Antarctic stable isotopic results. Proc. ODP, Sci. Results 113, 865–879.

– 1991: Abrupt deep-sea warming, palaeoceanographic changes and benthic extinctions at the end of the Palaeocene. Nature 353, 225–229.

KLUG, H.P. & ALEXANDER, L. 1974: X-ray Diffraction Procedures for Polycrystalline and Amorphous Materials. John Wiley and Sons, Inc., New York.

KOCH, P. L., ZACHOS, J. C. & GINGERICH, P. D. 1992: Correlation between isotope records in marine and continental carbon reservoirs near the Palaeocene/Eocene boundary. Nature 358, 319–322.

KOCH, P. L., ZACHOS, J. C. & DETTMAN, D. L. 1995: Stable isotope stratigraphy and paleoclimatology of the Paleogene Bighorn Basin (Wyoming, USA). Palaeogeogr. Palaeoclimatol. Palaeoecol. 115, 61–89.

KROOPNICK, P. 1985: The distribution of ^{13}C of TCO_2 in the world oceans. Deep Sea Res. 32, 57–84.

KÜBLER, B. 1983: Dosage quantitatif des minéraux majeurs des roches sédimentaires par diffraction X, Cahiers Inst. Géol. Neuch., Suisse, Série AX 1.1 & 1.2.

– 1987: Cristallinité de l'illite, méthodes normalisées de préparations, méthodes normalisées de mesures, Cahiers Inst. Géol. Neuch., Suisse, Série ADX.

LU, G. & KELLER, G. 1993: The Paleocene-Eocene transition in the Antarctic Indian Ocean: Inference from planktic foraminifera. Marine Micropaleontology 21, 101–142.

– 1995a: Planktic foraminiferal faunal turnovers in the subtropical Pacific during the Late Paleocene to Early Eocene. J. foram. Res. 25, 97–116.

– 1995b: Ecological stasis and saltation: species richness change in planktic foraminifera during the late Paleocene to early Eocene, DSDP Site 577. Palaeogeogr. Palaeclimatol. Palaeoecol. 117:211–227.

LU, G., KELLER, G., ADATTE, T. & BENJAMINI, C. 1995c: Abrupt change in the upwelling system along the southern margin of the Tethys during the Paleocene-Eocene transition event. Israel J. Earth Sci. 44:185–195.

LU, G. & KELLER, G. 1996: Separating ecological assemblages using stable isotope signals: late Paleocene to early Eocene planktic foraminifera, DSDP Site 577. J. foram. Res. 26(2):103–112.

LU, G., KELLER, G., ADATTE, T., ORTIZ, N. & MOLINA, E. 1996: Long-term (10^5) or short-term (10^3) $\delta^{13}C$ excursion near the Paleocene-Eocene transition: Evidence from the Tethys. Terra Nova 8:347–355.

MILLER, K. G., FAIRBANKS, R. G. & MOUNTAIN, G. S. 1987a: Tertiary oxygen isotope synthesis, sea level history, and continental margin erosion. Paleoceanography 2, 1–19.

MILLER, K. G., JANECEK, T. R., KATZ, M. E. & KEIL D. J. 1987b: Abyssal circulation & benthic foraminiferal changes near the Paleocene/Eocene boundary. Paleoceanography 2, 741–761.

MILLOT, G. 1970: Geology of clays. Springer-Verlag, Berlin 499 p.
MOORE, D. & REYNOLDS, R. 1989: X-Ray-diffraction and the identification and analysis of clay-minerals. Oxford University Press, 332 p.
OBERHÄNSLI, H. 1992: The influence of the Tethys on the bottom waters of the early Tertiary ocean. The Antarctic Paleoenvironment: A Perspective on Global Change (ed. by KENNETT, J. P.), Antarctic Research Series 56, 167–184.
OBERHÄNSLI, H. & HSÜ, K. J. 1986: Paleocene-Eocene paleoceanography. Mesozoic and Cenozoic Oceans, Geodynamics Series 15, 85–100.
O'CONNELL, S. B. O. 1990: Variations in upper Cretaceous and Cenozoic calcium carbonate precentages, Maud Rise, Weddell Sea, Antarctica. Proc. ODP, Sci. Results 113, 971–984.
O'CONNELL, S., CHANDLER, M. A. & RUEDY, R. 1996: Implications for the creation of warm saline deep water: Late Paleocene reconstructions and global model simulations. Geol. Soc. Amer. Bull. 108, 270–284.
ORTIZ, N. 1994: Mass extinction of benthic foraminifera at the Paleocene/Eocene boundary. Extinction and the fossil record (ed. by MOLINA, E.), Cuadernos interdisciplinares, Seminario Interdisciplinar Universidad Zaragoza 5, 201–218.
– 1995: Differential patterns of benthic foraminiferal extinction near the Paleocene-Eocene boundary in the North Atlantic and the western Tethys, Marine Micropaleontology, 26:341–359.
OWEN, R. M. & REA, D. K. 1985: Sea floor hydrothermal activity links climate to tectonics: The Eocene CO_2 greenhouse. Science 227, 166–169.
PAK, D. K. & MILLER, K. G. 1992: Paleocene to Eocene benthic foraminiferal isotopes and assemblages: implications for deepwater circulation Paleoceanography, 7, 405–422.
PEARSON, P. N., SHACKLETON, N. J. & HALL, M. A. 1993: Stable isotope paleoecology of middle Eocene planktonic foraminifera and multi-species isotope stratigraphy, DSDP Site 523, South Atlantic. J. foram. Res. 23, 123–140.
REA, D. K., ZACHOS, J. C., OWEN, R. M. & GINGERICH, P. D. 1990: Global changes at the Paleocene-Eocene boundary: climate and evolutionary consequences of tectonic events. Palaeogeogr. Palaeclimatol. Palaeoecol. 79, 117–128.
ROBERT, C. & CHAMLEY, H. 1991: Development of early Eocene warm climates, as inferred from clay mineral variations in oceanic sediments. Global and Planetary Change 89, 315–332.
– 1992: Paleocene and Eocene kaolinite distribution in the South Atlantic and Southern Ocean: Antarctic climate and paleoceanographic implications. Marine Geology 103, 99–110.
– 1994: Antarctic subtropical bumid episode at the Paleocene-Eocene boundary: Clay-mineral evidence. Geology 22, 211–214.
SCHMITZ, B., SPEIJER, R. P. & AUBRY, M. P. 1996: Latest Paleocene benthic extinction event on the southern Tethyan shelf (Egypt): Foraminiferal stable isotopic $\delta^{13}C$ and $\delta^{18}O$ records. Geology 24(4), 347–350.
SHACKLETON, N. J., CORFIELD, R. M. & HALL, M. A. 1985: Stable isotope data and ontogeny of Paleocene planktic foraminifera. J. foram. Res. 15, 321–336.
SINHA, A. & STOTT, L. D. 1994: New atmospheric PCO_2 estimates from palesols during the late Paleocene/early Eocene global warming interval. Global and Planetary Change 9, 297–307.
SLOAN, L. C. & BARRON, E. J. 1990: "Equable" climates during Earth history? Geology 18, 489–492.
– 1992: Eocene climate model results: Quantitative comparison to paleoclimatic evidence. Palaeogeogr. Palaeclimatol. Palaeoecol. 93, 183–202.
SLOAN, L. C., WALKER, J. C. G., MOORE, T. C. JR, REA, D. K. & ZACHOS, J. C. 1992: Possible methane-induced polar warming in the early Eocene. Nature 357, 320–322.
SLOAN, C. L. & THOMAS, E. in press: Global climate of the Late Paleocene: Modeling the circumstances associated with a climatic "event". in AUBRY, M-P., BERGGREN, W. A. & LUCAS, S., eds., The Paleocene/Eocene Boundary (IGCP Project 308), Eldigio Press.
SPEIJER, R. P. 1994: Extinction and recovery patterns in benthic foraminiferal paleocommunities across the Cretaceous/Paleogene and Paleocene/Eocene boundaries. Ph. D. thesis, Universiteit Utrecht, Geologica Ultraiectina 124, 191 p.
– 1994b: The late Paleocene benthic foraminferal extinction as observed in the Middle East. Bull. Soc. Belge Géol. 103 (3–4):267–280.
STOTT, L. D. 1992: Higher temperatures and lower oceanic PCO_2: a climate enigma at the end of the Paleocene Epoch. Paleoceanography 7, 395–404.
STOTT, L. D., SINHA, A., THIRY, M., AUBRY, M.-P. & BERGGREN, W. 1996: Global $\delta^{13}C$ changes across the Paleocene/Eocene boundary: Criteria for terrestrial-marine correlations. J. Geol. Soc. London, Spec. Publ. 101: 381–400.
THOMAS, E. 1990: Late Cretaceous through Neogene deep-sea benthic foraminifers (Maud Rise, Weddell Sea, Antarctica), Proc. ODP, Sci. Results 113, 571–594.
– 1992: Cenozoic deep-sea circulation: evidence from deep-sea benthic foraminifera, AGU Antarctic Research Series 56, 141–165.
THOMAS, E. & SHACKLETON, N. J. 1996: The latest Palaeocene benthic foraminiferal extinction and stable isotope anomalies. J. Geol. Soc. London, Spec. Publ. 101:401–441.
THOMAS, E. in press: Biogeography of the late Paleocene benthic foraminiferal extinction. In The Paleocene/Eocene Boundary, IGCP Project 308 (Ed. by AUBRY, M-P., BERGGREN, W. A. & LUCAS, S.). Eldigio Press.
WINDOM, H. L. 1976: Lithogenous material in marine sediments, in Chemical Oceanography, ed. by J. P. RILEY & R. CHESTER, Academic Press, New York, London 5, 103–135.
WING, S. L., BOWN, T. M. & OBRADOVICH, J. D 1991: Early Eocene biotic and climatic change in interior western America. Geology, 19, 1189–1192.
WING, S. L. & GREENWOOD, D. L. 1993: Fossils and fossil climate: The case for equable continental interiors in the Eocene, Phil. Trans.r. Soc. London, ser. B, 341, 243–252.
ZACHOS, J. C., LOHMANN, K. C., WALKER, J. C. G. & WISE, S. W. 1993: Abrupt climate change and transient climates during the Paleogene: a marine perspective. J. Geology 101, 191–213.
ZACHOS, J. C., STOTT, L. D. & LOHMANN, K. C. 1994: Evolution of early Cenozoic temperatures. Paleoceanography 9, 353–387.

Manuscript received April 15, 1997
Revision accepted June 23, 1998